

Water Movement during Internal Curing
Direct observation using X-ray microtomography

by

Dale P. Bentz ^a, Phillip M. Halleck ^b, Abraham S. Grader ^b, John W. Roberts ^c

**^a Building and Fire Research Laboratory National Institute of Standards and Technology,
Gaithersburg, MD**

^b Pennsylvania State University

^c Northeast Solite Corp

Reprinted from Concrete International, pp. 39 - 45, 2006.

**NOTE: This paper is a contribution of the National Institute of Standards and
Technology and is not subject to copyright.**

NIST

National Institute of Standards and Technology
Technology Administration, U.S. Department of Commerce

Water Movement during Internal Curing

Direct observation using X-ray microtomography

BY DALE P. BENTZ, PHILLIP M. HALLECK, ABRAHAM S. GRADER, AND JOHN W. ROBERTS

The goal of internal curing of concrete is to provide internal reservoirs that supply the hydrating cement paste with the water needed to maintain saturation within the paste's capillaries throughout the first days or weeks of hydration. It's been suggested that this water availability is especially critical during the first day of hydration in high-performance concretes, because without it, significant autogenous shrinkage and cracking can occur.^{1,2}

In this article, we discuss water movement during the internal curing of a high-performance mortar containing saturated lightweight aggregate (LWA). Using three-dimensional (3-D) X-ray microtomography with a voxel (in effect, a 3-D pixel) dimension of about 20 μm (0.0008 in.), we've been able to observe the emptying of individual pores within the LWA. For the mixture proportions employed in this study, much of the water initially in the LWA was removed within the first 24 hours of hydration at 30 °C (86 °F). The observations of water movement are supported by more conventional measures of performance, including degree of hydration based on loss-on-ignition measurements and compressive strength of mortar cubes.

TECHNOLOGIES FOR CHARACTERIZATION

In recent years, quantitative 3-D characterization of the microstructure of cement-based materials using X-ray computed tomography (CT) has become a reality.^{3,5} This technology is similar to computed axial tomography (CAT) scans used by the medical profession to view slices of the human body, but the X-ray intensity can be increased to provide better resolution without worrying about the harmful effects of higher radiation dosages.⁵ X-ray absorption techniques have also been successfully applied to examining water movement in cement-based materials during early-age curing.^{6,7} One application where such water movement is critical is internal curing of concrete.^{1,2,8,9} For successful internal curing, water contained in the internal reservoirs (LWA or superabsorbent polymer particles, for example) must readily evacuate the reservoirs to participate in the ongoing cement hydration reactions.

In this article, we show how X-ray CT is used to directly observe the migration of water from initially saturated LWA particles to the surrounding hydrating cement paste in a high-performance mortar throughout the first 2 days of isothermal 30 °C (86 °F) hydration. This application

TABLE 1:
MIXTURE PROPORTIONS FOR THE CONTROL AND
IC HIGH-PERFORMANCE MORTARS

Material	Control mortar, g (lb)	IC mortar, g (lb)
Cement	984.6 (2.17)	953.3 (2.10)
Water	344.6 (0.76)	333.7 (0.736)
Sand (total)	1870.7 (4.12)	1529.4 (3.37)
F95 fine sand	467.7 (1.03)	452.8 (0.998)
Graded sand (ASTM C 778 ⁽¹⁾)	355.4 (0.784)	344.1 (0.759)
20-30 sand (ASTM C 778 ⁽¹⁾)	355.4 (0.784)	287.8 (0.634)
S16 coarse sand	692.2 (1.53)	444.7 (0.980)
LWA (SSD)	—	185.5 (0.409)
Water in LWA	—	37.1 (0.082)

TABLE 2:
SELECTED SIZE DISTRIBUTION OF LWA USED IN
THE EXPERIMENTAL PROGRAM

Sieve size	Fraction retained
2.36 mm (No. 8)	0.000
2.00 mm (No. 10)	0.216
1.7 mm (No. 12)	0.166
1.18 mm (No. 16)	0.271
850 μm (No. 20)	0.201
600 μm (No. 30)	0.146
425 μm (No. 40)	0.000

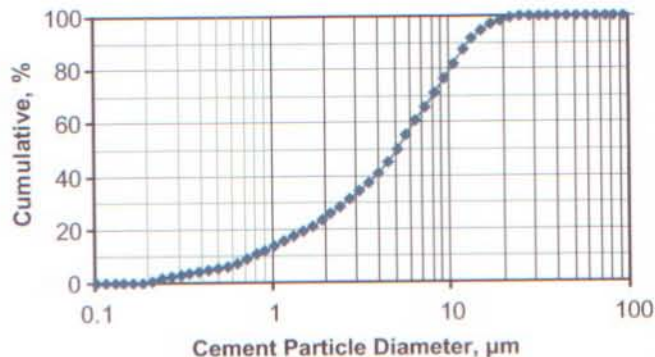


Fig. 1: Measured particle size distribution for the Type I/II portland cement used in the experiments ($1 \mu\text{m} = 3.94 \times 10^{-5} \text{ in.}$)

illustrates the power and potential of this experimental technique for examining dynamic processes occurring within the concrete microstructure. To supplement the X-ray CT observations, the performance of the mortar with internal curing was contrasted to that of a control mortar with respect to achieved degree of hydration and compressive strength development at ages up to 8 days.

MIXTURE PROPORTIONS

Mortars with a water-cement ratio (w/c) of 0.35 were prepared using an ASTM C 150¹⁰ Type I/II portland cement obtained from a local manufacturer. The cement had a measured specific gravity of 3.22 ± 0.01 and a potential Bogue composition of 66% tricalcium silicate, 12% dicalcium silicate, 6.5% tricalcium aluminate, and 11% tetracalcium aluminoferrite by mass. The particle size distribution of the cement, as measured by laser diffraction, is provided in Fig. 1. Both the control and the internally cured (IC) mortar contained a blend of four normalweight sands with a specific gravity of 2.61. This blend has been

shown to provide improved particle packing for high-performance mixtures. The complete mixture proportions for the two mortars are provided in Table 1.

To allow mixing in a conventional laboratory mixer, the expanded shale LWA was sieved to remove any particles retained on a 2.36 mm (No. 8) sieve. To avoid the presence of very fine LWA particles in the microtomography images, which could complicate their interpretation, LWA particles passing a 600 μm (No. 30) sieve were also removed. The specific gravity of the saturated surface-dry (SSD) sieved LWA was 1.7. The other four sands were also sieved (as necessary) to remove any particles retained on a 2.36 mm (No. 8) sieve or passing a 150 μm (No. 100) sieve. For the IC mortar, portions of the normal-weight 20-30 and S16 sands were replaced by equivalent volumes of LWA, consistent with the selected particle size distribution of the sieved LWA provided in Table 2.

The IC mortar was proportioned according to a previously outlined procedure that balances the water demand of the hydrating cement paste with the water supply from the SSD LWA.⁹ Thus, the necessary LWA mass was calculated as

$$M_{LWA} = \frac{C_f \cdot CS \cdot \alpha_{max}}{S \cdot \phi_{LWA}} \quad (1)$$

where

- M_{LWA} = mass of dry LWA required in mortar mixture, g (lb);
- C_f = cement content for mortar mixture, g (lb);
- CS = chemical shrinkage of cement, grams of water per gram of cement (lb of water per lb of cement);
- α_{max} = maximum expected degree of hydration of cement;
- S = degree of saturation of aggregate (0 to 1); and

ϕ_{LWA} = absorption of LWA, kilograms of water per kilogram of dry LWA (lb of water per lb of dry LWA).

The chemical shrinkage of the cement paste was directly measured using the ASTM C 1608 test method,¹² and a value of 0.06 grams of water per gram of cement (0.06 lb of water per lb of cement) was obtained when extrapolating to complete hydration. Throughout this study, curing at 30 °C (86 °F) was employed to accelerate the cement hydration reactions so the microtomography experiment could be completed in a reasonable 2 to 3 day time period. The absorption and desorption of the LWA were measured using a procedure similar to the ASTM C 1498 test method.¹³ A total SSD absorption of 25% by mass was measured for the sieved LWA, and 95% of this total absorbed water was removed when exposed to an environment with 93% relative humidity.

To examine whether pores in the LWA that had been emptied of water during hydration might function in a manner similar to air voids, we originally planned to freeze the microtomography specimen following the first few days of hydration to monitor internal water movement during freezing. Thus, the decision was made to only supply enough saturated LWA to maintain the saturation of the capillary pores in the hydrating cement paste during the first 3 days of hydration with a 1.1 safety factor. The measured degree of hydration, based on loss-on-ignition measurements,¹⁴ of a cement paste with 0.35 w/c cured under either saturated or sealed conditions at 30 °C (86 °F) is provided in Fig. 2. As expected, the degree of hydration of the saturated specimen exceeded that of the sealed one after 7 days of curing, due to the chemical shrinkage and self-desiccation accompanying the ongoing hydration in the sealed specimen. The degree of hydration obtained after 3 days was 0.56.

Substituting the values of $C_f = 953.3$ g (2.10 lb), $CS = 0.06$ g/g (0.06 lb/lb), $\alpha_{max} = 0.56$, $S = 0.25$, and $\phi_{LWA} = 0.95$ kg/kg (0.95 lb/lb) into Eq. (1) and applying the 1.1 safety factor results in a mass of dry LWA of 148.4 g (0.327 lb). Converting to a mass of SSD LWA results in the value of 185.5 g (0.409 lb) shown in Table 1. For the IC mortar, the LWA was presaturated overnight in a sealed plastic jar with the exact amount of water needed for its 25% SSD absorption capacity. The jar was shaken and rotated vigorously by hand on several separate occasions prior to the final preparation of the mortar.

Prior to the microtomography experiments, control and IC high-performance mortars were prepared in the National Institute of Standards and Technology (NIST) laboratory and cured under sealed conditions at 30 °C (86 °F). Their air contents were measured at 3% for the control mortar and 2% for the IC mortar, and 50 mm (2 in.) cubes were prepared for the measurement of compressive strength after 1, 3, and 8 days of sealed curing. After

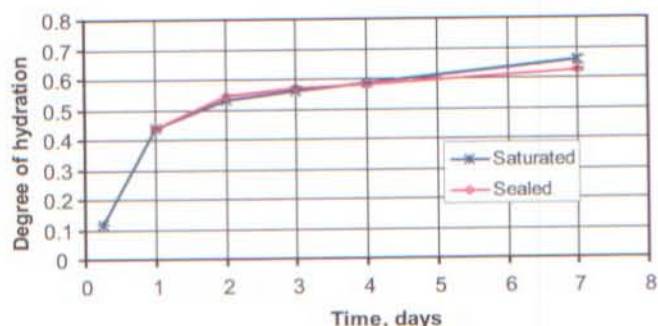


Fig. 2: Degree of hydration for cement paste with w/c = 0.35 hydrated under saturated or sealed curing conditions at 30 °C (86 °F)

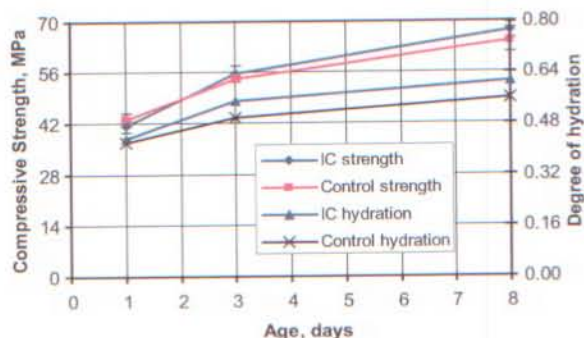


Fig. 3: Measured compressive strengths and degrees of hydration after 1, 3, and 8 days of sealed curing for the control and IC high-performance mortars. Error bars for compressive strength correspond to measured standard deviation in testing three cubes of each mortar mixture at each age (1 MPa = 145 psi)

breaking each set of cubes, the broken fragments of one cube from each mixture were retained for determination of the degree of hydration of the cement based on loss-on-ignition analysis, with an estimated uncertainty of 0.01.¹⁵

DEGREE OF HYDRATION AND COMPRESSIVE STRENGTH

The measured cube compressive strengths and degree of hydration are provided in Fig. 3. Two points are worth comment. First, the 1-day compressive strengths are already quite high at over 40 MPa (5800 psi). This is likely due to a combination of the optimized sand particle packing, the curing temperature of 30 °C (86 °F), and the somewhat unique particle size distribution of the cement (Fig. 1) that contained basically no particles larger than 30 μ m (0.0012 in.) in diameter. Second, IC is seen to clearly enhance hydration at 3 days and beyond and compressive strength after 8 days. The saturated conditions maintained within the hydrating cement paste 3-D microstructure by the water supplied in the IC reservoirs (LWA) lead to both more complete hydration

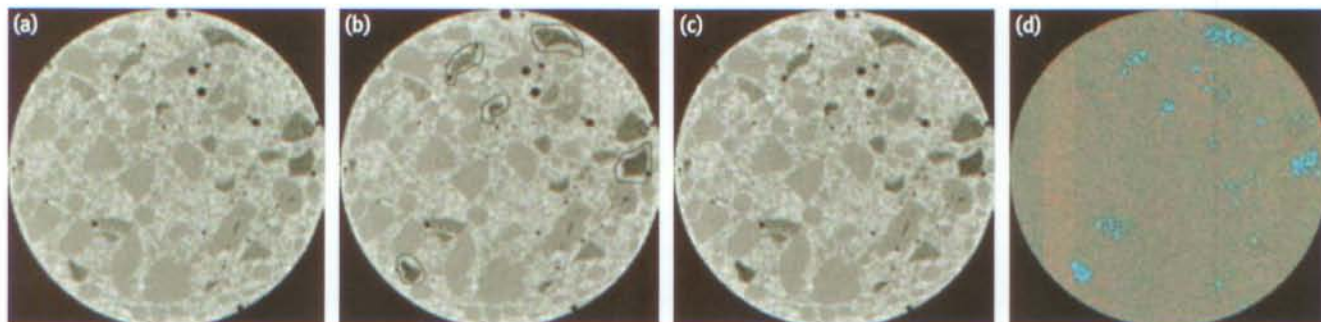


Fig. 4: Two-dimensional slices (13 x 13 mm [0.51 x 0.51 in.]) from 3-D microtomographic data sets corresponding to: (a) mortar immediately after mixing; (b) mortar after about 1 day of hydration; (c) mortar after about 2 days of hydration; and (d) color-coded original image subtracted from 1-day image. In the color-coded image, aqua indicates regions of drying and red indicates regions of wetting

and greater compressive strength development, as has been observed in previous studies.^{1,8}

X-RAY MICROTOMOGRAPHY

The IC mortar for the microtomography experiment was prepared in the microtomography laboratory at Pennsylvania State University using the procedures previously described. The prepared mortar was carefully compacted into a specimen holder consisting of a 13 mm (0.51 in.) inside diameter, 42 mm (1.65 in.) tall plastic tube. This tube was then sealed inside a larger 27 mm (1.06 in.) polypropylene tube in which a cooling fluid was constantly circulated (via a thermal bath) to maintain a constant fluid temperature of 30 °C (86 °F) throughout the hydration portion of the experiment. Following sample preparation, the specimen holder was placed inside the X-ray equipment. It remained basically stationary throughout the 57-hour experiment, except when being slowly rotated to collect the 3-D data sets. In this way, the images obtained after various hydration times could be easily and directly compared.

Volumetric X-ray CT data were collected using the facility's microfocus X-ray source with a voltage setting of 120 kV and a tube current of 200 μ A that minimized the focal spot size to about 10 μ m (0.0004 in.) and optimized the spatial resolution. For this study, all of the microtomography data sets were acquired with voxel dimensions 18 x 18 x 19 μ m (0.00071 x 0.00071 x 0.00075 in.), each of which was larger than the focal spot size. Each data set consisted of a 1024 x 1024 x 246 array of 16-bit X-ray absorption values on an arbitrary scale. Each of the 246 individual 2-D slices was available as a 16-bit TIFF format image for further processing. Eighty minutes were required for the collection of each complete 3-D data set.

Representative 2-D and 3-D views of the IC mortar microstructures as observed using X-ray microtomography are provided in Fig. 4 and 5, respectively. Four separate

microstructural components were clearly observed. From darkest to brightest, they were the air voids, the LWA particles, the normalweight sand grains, and the hydrating cement paste. For some of the LWA particles, individual (dark) empty pores were observed within the particle structure. By carefully comparing the images in Fig. 4(a) and 4(b), it was observed that the circled LWA particles had become darker between the original (after mixing) and the 1-day images. Also, in a few cases, new empty pores emerged within some of the circled LWA particles in the 1-day image. In contrast, little further change was observed between the 1- and 2-day images (Fig. 4(b) and 4(c), respectively), suggesting that most of the empty pores within the originally "saturated" LWA were created during the first day of hydration at 30 °C (86 °F). This was consistent with the time period when most of the measured hydration occurred, as indicated in Fig. 3.

In addition, it's worth noting that some empty pores were observed within the LWA particles even in the data set obtained just after mixing and casting of the specimen. There are two possibilities for these empty pores. The first is that the pores were empty within the SSD LWA particles that were added to the mortar mixture, either because they were inaccessible to an exterior source of water (isolated pores) or because the saturation method was only partially effective at filling all of the interconnected pores with water. The second possibility is that these empty pores were initially filled with water, but emptied during the initial mixing and casting of the specimen. In the future, a more quantitative analysis of the moisture contents of the individual LWA particles during the course of the hydration will be conducted to compare against the nominal 25% water absorption.

To quantitatively determine the locations where water was being drawn out of the LWA particles during the first day of hydration, a 3-D subtraction of the original data set from the 1-day data set was performed. First, random noise was removed from both data sets using a 5 x 5 x 5 median

filter where each voxel was replaced by the median value for all voxels within a 5 x 5 x 5 cube centered at the voxel being considered. The results of the 3-D subtraction are illustrated in Fig. 6 and 7. In Fig. 6, the aqua-colored regions correspond to those voxels where the largest negative difference was obtained. The differences are negative because an empty pore has an X-ray absorption signal that is significantly less than that of a water-filled one. In Fig. 7, these same aqua regions are superimposed on a magnified portion of one 2-D slice from the original microtomography data set, allowing direct verification that the aqua regions are generally contained within the boundaries of the LWA particles. Also, in Fig. 6 and 7, the shapes of some of the newly emptied pores (highlighted in aqua) within several of the LWA particles can be readily observed.

While it's relatively straightforward to detect the water leaving the SSD LWA during hydration using the X-ray microtomography technique, it's not possible to isolate where the water goes. At early ages, due to the high permeability of the hydrating cement paste, water is able to move rapidly over a distance of at least several millimeters.^{6,16} Thus, it would be expected that the hydrating cement paste would remain saturated within a distance of at least 2 mm (0.079 in.) from an internal reservoir. Simulations of this water availability distribution were conducted using programs¹⁷ similar to those available for free at <http://ciks.cbt.nist.gov/lwagg.html>, and the resulting simulated spatial distribution of water availability is shown in Fig. 8.

From the 3-D simulation that incorporated the IC mortar mixture proportions and LWA particle size distribution provided in Table 1 and 2, 97% of the total cement paste volume was found to be within a 2 mm (0.079 in.) distance of the surface of an LWA particle. This supports the observation that the water coming from the LWA internal reservoirs is basically uniformly redistributed throughout the entire 3-D mortar microstructure, so that no regions of increased brightness (density) were readily isolated in the microtomography data sets.

For example, in Fig. 4(d), the voxels with the largest positive difference between the 1-day hydration and the original microstructure data sets (indicating those regions that had undergone the greatest increase in density by imbibing the most water) are highlighted in red. These quite small red regions were homogeneously distributed throughout the entire specimen. At later ages (28 days and beyond), as the permeability of the cement paste decreases by several orders of magnitude, water movement may become limited to distances of 100 to 200 μm (0.004 to 0.008 in.),¹⁸ and one might expect to observe brighter hydration rims around the LWA particle reservoirs in IC mortars with sufficient volumes of internal curing water.

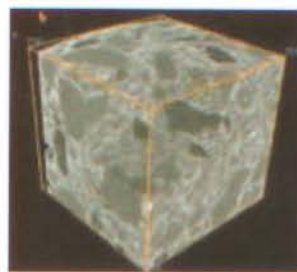


Fig. 5: Three-dimensional image (4.6 x 4.6 x 4.7 mm [0.181 x 0.181 x 0.185 in.]) of a portion of the microtomography data set for the IC mortar obtained immediately after mixing and casting

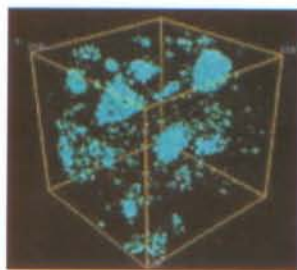


Fig. 6: Three-dimensional color-coded image of original data set subtracted from that obtained after 1 day of hydration. Aqua-colored volumes indicate regions where the LWA particles had lost water to the surrounding hydrating cement paste. The 3-D volume is 4.6 x 4.6 x 4.7 mm (0.181 x 0.181 x 0.185 in.)



Fig. 7: Two-dimensional image (4.6 x 4.6 mm [0.181 x 0.181 in.]) of a portion of the original mortar microstructure with the locations of the evacuated water (in aqua) superimposed

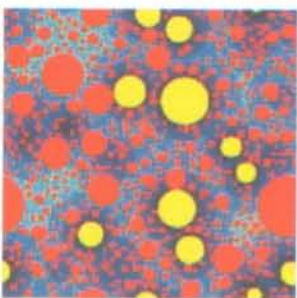


Fig. 8: Two-dimensional slice from three-dimensional simulated water availability distribution for IC mortar. Image size is 10 x 10 mm (0.39 x 0.39 in.); red indicates normalweight sand, yellow indicates LWA, and concentric rings of various shades of blue indicate hydrating cement paste within 0.1, 0.2, 0.3, 0.5, 1.0, and 2.0 mm (0.004, 0.008, 0.012, 0.02, 0.04, and 0.08 in.) of an LWA surface, respectively

PROSPECTUS

The power and potential of applying X-ray microtomography to quantitatively visualize dynamic processes within cement-based materials has been demonstrated for the case of water movement during the internal curing of a high-performance mortar. Clear evidence was observed that many of the initially water-filled pores within the SSD LWA particles empty during the first day of hydration (the critical time window for avoiding early-age cracking).¹² These observations were supported by conventional measures of the degree of hydration and compressive strength development of companion mortar specimens. The X-ray microtomography technique

ONE NAME
IN TILT-UP BONDBREAKERS
STANDS ABOVE
THE COMPETITION.

SILCOSEAL

Nox-Crete has been a trusted name in concrete construction chemicals since 1956. In the 1970s, we introduced the first generation of **Silcoseal** cure and bondbreakers and have been setting the industry standard for performance ever since.

The same quality and performance can be found in our fully compatible line of **Tilt-Up Partner Products**:

Silcoseal
Tilt-Up Cure &
Bondbreakers

Duro-Nox
Liquid Silicate
Floor Hardener

Dynaflex
Semi-Rigid Epoxy
& Polyurea
Joint Fillers

Panel Patch
Exterior Wall
Surfacing
Compound

Duro-Polish
Slip-Resistant
Floor Polish

Nox-Carb
Exterior Wall
Finish

100% Compatibility
GUARANTEE



When you choose the integrated chemical solutions of our **Tilt-Up Partner Products**, all it takes is one call to be connected to some of the best technical support people in the industry. Call us today to find out more.

(800) 669-2738

nox-crete.com

50
1956 2006

nox-crete

chemical solutions to concrete problems

CIRCLE READER CARD #8

should be equally applicable to other internal curing materials, such as superabsorbent polymers or water-absorptive fibers.

It had been planned to extend the current experiment by freezing the specimen to observe whether water returns from the hydrating cement paste into the pores within the LWA (and the air voids) during the expansive ice formation process. Unfortunately, it was not possible to decrease the temperature of the specimen lower than about -8°C (17.6°F), which is in the range where freezing may not have occurred within the mortar microstructure due to supercooling effects. In the future, it would be interesting to repeat the experiment with equipment that can achieve a lower temperature on the order of -20°C (-4°F), at which point the water within the percolated capillary pores of the hydrating cement paste should have definitely frozen.

Acknowledgments

The authors would like to thank M. Peltz and J. Winpiger of the Building and Fire Research Laboratory at the National Institute of Standards and Technology for their assistance with materials characterization and specimen preparation. They would also like to thank J. Hook of the Lehigh Portland Cement Co. for supplying materials for this study and M. Juenger of the University of Texas at Austin for a careful review of the manuscript.

References

1. Cusson, D., and Hoogeveen, T., "Internally Cured High-Performance Concrete Under Restrained Shrinkage and Creep," *CONCREEP 7 Workshop on Creep, Shrinkage and Durability of Concrete and Concrete Structures*, Nantes, France, Sept. 12-14, 2005, pp. 579-584.
2. Cusson, D.; Hoogeveen, T.; and Mitchell, L.D., "Restrained Shrinkage Testing of High-Performance Concrete Modified with Structural Lightweight Aggregate," *7th International Symposium on Utilization of High-Strength/High-Performance Concrete*, Washington, DC, June 2005, 20 pp.

3. Bentz, D.P.; Mizell, S.; Satterfield, S.; Devaney, J.; George, W.; Ketcham, P.; Graham, J.; Porterfield, J.; Quenard, D.; Vallee, F.; Sallee, H.; Boller, E.; and Baruchel, J.; "The Visible Cement Data Set," *Journal of Research of the National Institute of Standards and Technology*, V. 107, No. 2, Mar. 2002, pp. 137-148.

4. Garboczi, E.J., "Three-Dimensional Mathematical Analysis of Particle Shape Using X-ray Tomography and Spherical Harmonics: Application to Aggregates used in Concrete," *Cement and Concrete Research*, V. 32, No. 10, Oct. 2002, pp. 1621-1638.

5. Garci Juenger, M.C., "X-ray Vision for Cement-Based Materials," *Concrete International*, V. 26, No. 12, Dec. 2004, pp. 38-41.

6. Bentz, D.P., and Hansen, K.K., "Preliminary Observations of Water Movement in Cement Pastes During Curing Using X-ray Absorption," *Cement and Concrete Research*, V. 30, No. 7, July 2000, pp. 1157-1168.

7. Bentz, D.P.; Geiker, M.R.; and Hansen, K.K., "Shrinkage-Reducing Admixtures and Early Age Desiccation in Cement Pastes and Mortars," *Cement and Concrete Research*, V. 31, No. 7, July 2001, pp. 1075-1085.

8. Geiker, M.R.; Bentz, D.P.; and Jensen, O.M., "Mitigating Autogenous Shrinkage by Internal Curing," *High Performance Structural Lightweight Concrete*, SP-218, J.P. Ries and T.A. Holm, eds., American Concrete Institute, Farmington Hills, MI, 2004, pp. 143-154.

9. Bentz, D.P.; Lura, P.; and Roberts, J.W., "Mixture Proportioning for Internal Curing," *Concrete International*, V. 27, No. 2, Feb. 2005, pp. 35-40.

10. ASTM C 150-05, "Standard Specification for Portland Cement," ASTM International, West Conshohocken, PA, 2005, 8 pp.

11. ASTM C 778-02, "Standard Specification for Standard Sand," ASTM International, West Conshohocken, PA, 2002, 3 pp.

12. ASTM C 1608-05, "Standard Test Method for the Chemical Shrinkage of Hydraulic Cement Paste," ASTM International, West Conshohocken, PA, 2005, 4 pp.

13. ASTM C 1498-04a, "Standard Test Method for Hygroscopic Sorption Isotherms of Building Materials," ASTM International, West Conshohocken, PA, 2004, 4 pp.

14. Bentz, D.P., "Three-Dimensional Computer Simulation of Cement Hydration and Microstructure Development," *Journal of the American Ceramic Society*, V. 80, No. 1, Jan. 1997, pp. 3-21.

15. Bentz, D.P., "Capitalizing on Self-Desiccation for Autogenous Distribution of Chemical Admixtures in Concrete," *Proceedings of the 4th International Seminar on Self-Desiccation and Its Importance in Concrete Technology*, B. Persson, D.P. Bentz, and L.-O. Nilsson, eds., Lund University, Lund, Sweden, 2005, pp. 189-196.

16. Lura, P.; Bentz, D.P.; Lange, D.A.; Kovler, K.; Bentur, A.; and van Breugel, K., "Measurement of Water Transport from Saturated Pumice Aggregates to Hardening Cement Paste," *Materials and Structures*, 2006, in press.

17. Bentz, D.P.; Garboczi, E.J.; and Snyder, K.A., "A Hard Core/Soft Shell Microstructural Model for Studying Percolation and Transport in Three-Dimensional Composite Media," *NISTIR 6265*, U.S. Department of Commerce, 1999, 51 pp.

18. Bentz, D.P., and Snyder, K.A., "Protected Paste Volume in Concrete: Extension to Internal Curing Using Saturated Lightweight

Fine Aggregate," *Cement and Concrete Research*, V. 29, No. 11, Nov. 1999, pp. 1863-1867.

Received and reviewed under Institute publication policies.



ACI member **Dale P. Bentz** is a Chemical Engineer in the Materials and Construction Research Division, National Institute of Standards and Technology (NIST), Gaithersburg, MD. He is a member of ACI Committees 231, Properties of Concrete at Early Ages; 236, Material Science of Concrete; and 308, Curing Concrete. His research interests include experimental and computer modeling studies of the microstructure and performance of cement-based materials.



Phil Halleck is an Associate Professor of Energy and Geoenvironmental Engineering. He has worked on geotechnical research projects at the Los Alamos National Laboratory, Schlumberger, TerraTek, and Pennsylvania State University. He received a BA in chemistry and a PhD in geophysics from the University of Rochester and the University of Chicago, respectively. His research interests include the use of X-ray CT to observe fluid flow and saturation in stressed rock, soils, and other porous media.



Abraham Grader is a Professor of Petroleum and Natural Gas Engineering at Pennsylvania State University. He received a BSc from the Technion, Israel Institute of Technology, and an MSc and a PhD from Stanford University. His research interests include well testing, reservoir engineering, and multi-phase fluid flow in porous media, including pore-scale characterization using high-resolution X-ray CT.



ACI member **John W. Roberts** is Chairman of Northeast Solite Corp. He is a member of ACI Committees 224, Cracking; 308, Curing Concrete; 325, Concrete Pavements; and 362, Parking Structures.